# Analytical and Numerical Verification of Vibration Design in Timber Concrete Composite Floors

**Perković, Nikola; Rajčić, Vlatka; Barbalić, Jure**



forests

MDPI

*Article*

# Analytical and Numerical Verification of Vibration Design in Timber Concrete Composite Floors

**Nikola Perković *, Vlatka Rajčić and Jure Barbalić**

Structural Department, Faculty of Civil Engineering, University of Zagreb, 10000 Zagreb, Croatia; vlatka.rajcic@grad.unizg.hr (V.R.); jure.barbalic@grad.unizg.hr (J.B.)
* Correspondence: nikola.perkovic@grad.unizg.hr

**Abstract:** The TCC concept has been studied and developed over the past decades. The variety of solutions shows the meaningfulness and functionality of this system, as well as the continuous work of scientists over time. To benefit from these advantages, the composite needs to provide sufficient stiffness to meet the serviceability criteria and load capacity to resist loading at every stage of the building life. An example of connector types and load slip curves according to EN 1995 is given. This paper discusses possible limitations related to residential areas, and additionally, the possible solutions that EN 1995 does not discuss in the case of resonant response ($f_1 < 8$ Hz). The theoretical studies were accompanied by numerical analyses considering certain simplifications suitable for practical use.

**Keywords:** timber; concrete; composite; connection; stiffness; vibration; acceleration; FEM



**Citation:** Perković, N.; Rajčić, V.; Barbalić, J. Analytical and Numerical Verification of Vibration Design in Timber Concrete Composite Floors. *Forests* **2021**, *12*, 707. https://doi.org/10.3390/f12060707

Academic Editors: Miroslav Premrov, Vesna Žegarac Leskovar and Angela Lo Monaco

Received: 29 March 2021
Accepted: 24 May 2021
Published: 29 May 2021



## 1. Introduction

The composite system based on concrete and timber represents a very successful engineering solution in the process of optimization of construction. The timber–concrete composites (TCC) date back to the beginning of the 20th century. The first scientific approach was applied to the system of nails and steel braces as connectors between the concrete slab and timber beams, patented by Müller in 1922 [1]. However, it has been widely used only in the last 30 years [2], when it proved to be a good solution for the renovation of existing timber floors due to today's code requirements of load-bearing capacity, deformability, vibration, fire and earthquake resistance, and sound insulation [3]. Moreover, due to the conditions of overcoming larger spans without the use of walls (pillar–slab or frame–slab system), as well as the requirement for the floor structure to be a rigid diaphragm, it has become a must-have solution in the design of tall timber buildings [4–9]. The advantages of TCC construction in the building industry are achieved through the mass of concrete, compared with timber floors, as well as on the positive characteristics of the wood (high tensile strength) and concrete (high compressive strength). The disadvantages, on the other side, could be found in greater dead loads, which results in higher manufacturing and assembly demands. Analysis of the possible application of TCC is given in [10,11].

Economic considerations of the cost-effectiveness of TCC given by [12] tried to estimate market opportunities and obstacles when using TCC. Through the questioning of experts, it provided a prognosis and assessment of the market potentials for TCC in Germany based on a realistic scenario. The scenario presented in [12] results in a potential floor area for TCC for multistorey residential construction, single and two-family house construction, and nonresidential building. Altogether, a potential of approx. 1.6 million $m^2$ is the result (the market figures are based on Germany in 2014). The establishment of TCC for the wood-based sector makes significantly higher demands than what would normally occur with technical innovations where TCC has a considerable impact on the identity of building with wood. Such an approach to the market requires conditions that will bring the

benefits of TCC closer to the user, with a sense of comfort being one of the most important factors. Therefore, the vibration conditions, or the way of the connection (between wood and concrete) principles which defined them, become the main accent in the design of floor structures.

The usage of optimization in product development is growing as both computational capabilities and newly developed numerical algorithms are increasing. At the same time, all design problems have more than one conflicting objective in design optimization, and these objectives need to be integrated to yield one final design. Thus, the design problem can be formulated as a multi-objective optimization problem [13]. In the serviceability design of the TCC floor, the evaluation index plays a critical role, which makes it essential to check the vibration behavior and occupant comfort. In this paper, two objectives of the cost and demanded function and comfort of the use of the TCC floor system have been chosen as two capital objectives. To achieve a well-engineered TCC floor design, a framework based on optimal design variables include the optimized thickness of the concrete and the optimized smeared stiffness of connectors, which are considered regarding the TCC floor structure vibrations.

FEA parametric analysis was performed to obtain the fundamental frequency of the composite floor with different types of connectors, different concrete slab thicknesses, and two types of span (short- and large-span system) for the usual type of boundary conditions (simply supported). Based on the numerical analysis, three existing analytical models were applied to estimate the correlation of fundamental frequency results. Conclusions are given on the optimal design of the elements.

## 2. TCC Floor System Subjected to Footfall Induced Vibration

Analysis of TCC floors in the area of serviceability, besides vibration, is developing progressively due to the increasing application of larger spans [14]. As vibrations performance depends on the floor system mass, the longitudinal and transverse bending stiffness, the damping of the floor system, and the shear stiffness of the joints between timber and concrete, changing each of these parameters will affect the dynamic response. The influence of the cracks developing in the concrete slab and the deflections of the supporting beams are also considered as one of the influencing parameters. At present, plenty of studies focus on such dynamic characteristics as natural frequencies, damping ratios, and mode shapes of TCC floor systems; in among the others mentioned here, there are more studies [15–27]. If a fixed-length system is considered, it can be concluded that the thickness of the concrete slab contributes to stiffness as well as mass, but the increased mass can outweigh the improvement to stiffness, thus causing the fundamental frequency to decrease. Furthermore, short-span systems (up to 6 m) determine acceptable dynamic responses to footfall-induced vibration, since such floors usually have sufficient transversal bending stiffness with natural eigenfrequency above 8 Hz. However, with the large-span length (above 6 m), the floors' natural eigenfrequency usually does not meet the requirements above 8 Hz [28].

According to [29] for floor performance levels I–VI, no further investigations are necessary if the requirements in respect to fundamental frequency, acceleration or velocity, and stiffness from Table 1 are satisfied. The root mean square acceleration or velocity responses are compared to the vibration perception base curve in [30]. The acceleration criterion is expressed as a multiple of the base curve value. This multiple is termed as the response factor $R$ (equal to mean square velocity response $v_{rms}/0.0001$) given in Table 1. For resonant vibration design situations, (when $f_1 < 8$ Hz), the minimum fundamental frequency, acceleration, and stiffness criteria of Table 1 should be fulfilled. For transient vibration design situations, (when $f_1 \geq 8$ Hz), the velocity and stiffness criteria of Table 1 should be fulfilled.

**Table 1.** Floor vibration criteria according to floor performance level.

| Criteria | Floor Performance Levels | | | | | | |
|---|---|---|---|---|---|---|---|
| | **I** | **II** | **III** | **IV** | **V** | **VI** | **VI** |
| stiffnes criteria $w_{1kN}$ [mm] $\leq$ | 0.25 | 0.25 | 0.50 | 0.80 | 1.20 | 1.60 | no criteria |
| response factor R $\leq$ | 4 | 8 | 12 | 16 | 24 | 32 | |
| frequency criteria $f_1$ [HZ] $\geq$ | 4.50 | | | | | | |
| acceleration criteria $a_{rms}$ [m/s$^2$] $\leq$ | 0.005R | | | | | | |
| velocity criteria $v_{rms}$ [m/s] $\leq$ | 0.0001R | | | | | | |

A structure with timber–concrete composite parts should be designed and constructed such that all relevant serviceability limit states are satisfied according to the principles of [31], where criteria are stated in Subclause 3.4 of [31]. The dynamic properties of floor beams, then, should satisfy the criteria of Subclause 1.4.4 of [31]. Lightweight (timber/wood) structures with a span length below approximately 6 to 8 m, and heavy (concrete) floors "with short span" are related to the high-frequency, while the low-frequency floor includes heavyweight floors with a longer span [32]. The vibration level, according to [33], should be estimated by measurement or by calculation, taking into consideration the expected stiffness of the member, component, or structure, and the modal damping ratio. Residential floor structures have often been treated as either low- or high-frequency floors, where suggestions for limits of vibration are given in Subclause 7.3 of [34]. People most often feel discomfort at floor frequencies between 4 and 8 Hz, which corresponds to the natural frequencies of some organs of the human body [35,36]. Therefore, the authors of [34] recognized that, in case of a fundamental frequency that is less than 8 Hz, a special investigation should be made, and, if a fundamental frequency is greater than 8 Hz, the following requirements should be satisfied:

$$w/F \leq a, \text{ in mm/kN}, \quad (1)$$

$$v \leq b^{(f1/\varsigma)}, \text{ in m/Ns}^2, \quad (2)$$

where w is the maximum instantaneous vertical deflection caused by a vertical concentrated static force F applied at any point on the floor, taking account of load distribution, v is the unit impulse velocity response, i.e., the maximum initial value of the vertical floor vibration velocity (in m/s) caused by an ideal unit impulse (1 Ns) applied at the point of the floor giving the maximum response (according to the [34], components above 40 Hz may be disregarded), and $\varsigma$ is the modal damping ratio. These calculations should be made under the assumption that the floor is unloaded, i.e., only the mass corresponding to the self-weight of the floor and other permanent actions.

For a rectangular floor with an overall length dimension of l and width b, simply supported along all four edges and with timber beams having a span e, the natural undamped eigenfrequency $f_1$ may approximately be calculated as:

$$f_1 < \pi/(2l^2)\sqrt{((EI)_l/m)}, \text{ in Hz}, \quad (3)$$

where m is the mass per unit area in kg/m$^2$, l is the floor span in m, and $(El)_l$ is the equivalent plate bending stiffness of the floor about an axis perpendicular to the beam direction in Nm$^2$/m. The concrete slab in timber–concrete composite systems is relatively narrow compared to pure concrete slabs. Therefore, the reinforcement is often installed near the centroid of the cross-section. The cracking of concrete will lead to a significant drop in the bending stiffness. The effective width is caused by the distribution of the

normal force in the concrete cross-section as a shell and the distribution of the bending moment as a plate. Due to the decrease of the bending stiffness by cracking, the load distribution in the concrete slabs tends to be only in the shell model. However, the effective width given in [37] is comparable to the shell mode, whereas in [38], the plate mode is also considered [33,39,40]. For that reason, it is appropriate to use the effective width according to [37] instead of [38].

Considering the need to simplify the calculation, the composite floor can be considered as a parallel arrangement of composite beams. The equation above can be represented as:

$$f_1 < \pi/(2l^2)\sqrt{(((EI)_{ef}/b_c)/m)}, \text{ in Hz}, \quad (4)$$

where $b_c$ is the spacing between the timber beams [32]. The natural frequencies of the composite beams and the spacing of the composite beams are the same as those of the composite floor [41]. For the same type of floor, the value v may, as an approximation, be taken as:

$$v \leq 4(0.4 + 0.6n_{40})/(mbl + 200), \text{ in } m/Ns^2, \quad (5)$$

where v is the unit impulse velocity response in $m/(Ns^2)$, m is the mass in $kg/m^2$, b is the floor width in m, l is the floor span in m, and $n_{40}$ is the number of first-order modes with natural frequencies up to 40 Hz which may be calculated from:

$$n_{40} \leq (((40/f_1)^2 - 1)((b/l)^4)((EI)_l/(EI)_b))^{0.25}, \quad (6)$$

where $(EI)_b$ is the equivalent plate bending stiffness, in $Nm^2/m$, of the floor about an axis parallel to the beams, where $(E1)_b < (EI)_l$. Series of studies and research, of which the results are given in [42–49], were a background for choosing values for the appropriate modal damping ratio. According to [33], for floors, unless other values are proven to be more appropriate, a modal damping ratio of $\varsigma = 0.025$ (i.e., 2.5%) should be used for timber–concrete composite slabs alone and $\varsigma = 0.035$ slabs with a floating screed. The instantaneous elastic bending stiffness of the composite structure should be used in vibration analysis. Alternatively, damping ratio values can be calculated based on actual loads (i.e., precomposite dead load, postcomposite dead load, and sustained live load) [50]. More accurate damping values can alternatively be obtained by samples testing, applying [51].

At present, some other proposed models for the natural frequencies occurred. The authors of [52] proposed Equation:

$$f_1 < 1/(2\pi\sqrt{(g/y_w)}), \text{ in Hz}, \quad (7)$$

where $y_w$ is the weighted average of the static deflection of the beam due to the self-weight of the floor or the dead weight of the beam–slab system, and g is the gravitational acceleration. A similar method is proposed in [53], where the fundamental frequency of simply supported beams or floor systems under uniformly distributed additional loads, as shown in the equation:

$$f_1 < (\pi/2)\sqrt{((gEI)/(wl^4))}, \text{ in Hz}, \quad (8)$$

where E is Young's modulus of the beam, I is the moment of inertia of the beam, w is the uniform load per unit length, and l is the span. For the bending stiffness of composite beams with pinned boundary conditions, the $\gamma$-method determined in [33] should be used.

The effective stiffness of the partially composite beam is calculated as follows:

$$EI_{ef} = E_c(I_c + \gamma_c A_c a_c^2) + E_t(I_t + \gamma_t A_t a_t^2), \text{ in } Nmm^2, \quad (9)$$

where subscripts c and t refer to concrete and timber elements, respectively, E is Young's modulus of the material, A and I are the area and the second moment of area of the element

cross-section, a is the distance from the centroid of the element to the neutral axis of the composite section, and $\gamma$ is the shear connection reduction factor according to:

$$\gamma_c = 1/(1 + (\pi^2 E_c A_c s)/(K_{ser} l^2)), \quad (10)$$

$$\gamma_t = 1, \quad (11)$$

where s is the spacing of the connectors assumed as smeared along the span, l is the span, and $K_{ser}$ is the slip modulus of the connector. The authors of [54] proposed a method to calculate the effective stiffness of composite beam with an arbitrary boundary as:

$$EI_{ef} = EI_\infty/(1 + (EI_\infty/EI_0 - 1)/(1 + ((\mu/\pi)^2)((\alpha/L)^2))), \text{ in } Nmm^2, \quad (12)$$

where $\mu$ is the buckling length factor, r is the distance between the centroid of timber section to the centroid of the concrete section, $\alpha$ is the nondimensional composite action (shear connector) parameter, $EI_0$ the bending stiffness of the noncomposite section ($K \to 0$), and $EI_\infty$ is the bending stiffness of the fully composite section. $EA_0$ and $EA_p$ are the sum and product of axial stiffness of the sub-elements, respectively. Some design methods, such as the $\gamma$-method, assume that the connectors may be smeared along the beam axis. In this case, no discrete connector is considered, but the stiffness per unit length is taken into account. For short distances, this simplification works quite well. However, with increasing distance, the discrete connector leads to local stresses. This conclusion is reported in [55,56]. The authors of [55] propose a maximum distance of 5%, whereas [56] proposes a maximum distance of 3%. For notches as the connection between timber and concrete, [57] proposes an effective distance in order to enable smearing of these connectors. Providing that the effective spacing of the connections is less than or equal to 5% of the distance between the points of contra flexure, even distribution of the connection stiffness along the beam axis (smearing) may be used. If the spacing of the connections is greater than 5% of the distance between the points of contra flexure, then, when smearing, the connections should be distributed in proportion to the shear force. Comparing the sinusoidal course and the constant course of the normal force, the different deformation can be evaluated. In the hyperstatic composite cross-section, the stiffness influences the distribution of the forces. The stiffness of the cross-section connected with discrete connectors should be reduced by the factor $2/\pi$ to consider the same stiffness as in the smeared case. For the reason of simplification, this factor is rounded to 0.7, since the case of only one single connector at each of the beams is hardly used. However, up to now, no other values are given, since the variability of possible positions of the connectors is quite large. So, in the absence of a more precise model, only 70% of the axial stiffness of the attached cross-section should be considered for the calculation of stresses and deformation. For the calculation of the shear force in the connection, 100% of the axial stiffness of the cross-section should be considered [33]. If the spacing and/or stiffness of the connections are varied in proportion to the shear force, the effective spacing may be determined as:

$$s_{ef} = 0.75 s_{min}(K_{ref}/K_{max}) + 0.25\, s_{max}(K_{ref}/K_{min}), \text{ in mm}, \quad (13)$$

where $s_{ef}$ is the effective spacing of the connections, $s_{min}$ is the minimum spacing of the connections, $K_{ref}$ is the reference stiffness of the connection used with the corresponding value of $s_{ef}$, $K_{max}$ is the maximum stiffness of the connection, $K_{min}$ is the minimum stiffness of the connection, and $s_{max}$ is the maximum spacing of the connections or the maximum distance between the connection and the point of zero shear force.

The slip modulus for serviceability limit states that $K_{ser}$ of connections made with dowel-type fasteners inserted perpendicular to the shear plane should be determined using:

$$K_{ser} = 2(\rho_m{}^{1.5})d/23, \text{ in N/mm}, \quad (14)$$

for dowels, bolts, screws, and nails (with predrilling), and nails (without predrilling):

$$K_{ser} = 2(\rho_m{}^{1.5})(d^{0.9})/30, \text{ in N/mm}, \quad (15)$$

where $K_{ser}$ is the slip modulus for serviceability limit states, $\rho_m$ is the mean value of the timber member density in kg/m$^3$, and d is the fastener diameter in mm. Research studies [58–61] show that this can be a good estimation when more detailed data is not available. For regular interlayers, with stiffness perpendicular to the shear plane similar to that of timber and with thickness up to 30 mm, the slip modulus of connections with dowel-type fasteners may be taken as that for a similar configuration without an interlayer, with a reduction of 30% [11]. In other cases where there is an intermediate nonstructural layer between the timber and the concrete, the slip modulus should be determined by tests or special analysis. For connections made with steel rebar glued into timber perpendicular to the shear plane using epoxy resin, the slip modulus for serviceability limit states $K_{ser}$ should be determined according to:

$$K_{ser} = 0.10E_{tim}d, \text{ in N/mm}, \quad (16)$$

where $E_{tim}$ is the mean modulus of elasticity of timber parallel to the grain in N/mm$^2$, and d is the nominal diameter of the rebar in mm [33,58,60,62]. In many cases, when the manufacturer provides new, modern types of connectors, such as [63], slip modulus should be determined based on verified tests. For notched connections, the slip modulus for serviceability limit states that $K_{ser}$ should be determined according to:

$$K_{ser} = 1000 \text{ N/mm/mm for } h_n = 20 \text{ mm}, \quad (17)$$

$$K_{ser} = 1500 \text{ N/mm/mm for } h_n \geq 30 \text{ mm}, \quad (18)$$

where $h_n$ is the depth of the notch. Linear interpolation may be used for $h_n$ between 20 mm and 30 mm [33,64].

By using the effective bending stiffness expressed above, three different calculation models have been combined as a function of the two design variables: concrete thickness hc and overspread connector stiffness $K_{ser}/s$, where s is spacing between connectors, and $K_{ser}/s$ is stiffness per unit length of the element expressed in (N/mm)/mm. By applying the deflection criteria, the minimum bending stiffness fulfilling the eigenfrequency criteria can be predicted.

## 3. FEM Analysis of TCC Floor Slab

Numerical modeling is a powerful tool aimed at expanding knowledge and saving time and, ultimately, finance. Efficient data input and intuitive handling facilitate the modeling of simple and large structures. The numerical analyses aimed to extend the knowledge of the behavior of the tested system. Furthermore, the numerical simulations served to confirm and complement the experimental results. In this paper, the RFEM program is used, a powerful 3D FEA program helping structural engineers meet requirements in modern civil engineering. One such case is certainly composite systems, specifically, timber–concrete systems. An additional aggravating circumstance is defining and calculating a semi-rigid connection between the different elements and materials. There are several options to calculate a semi-rigid composite beam or floor. The main difference is in the modeling method itself. Some methods ensure simple modeling (such as the gamma method). However, there are other more complex methods (shear analogy). Another option for modeling a composite system is shown in this paper. Since the definition and analysis of connecting elements are time-consuming, it is recommended to connect the surfaces of the elements to the other surfaces directly. Although there are several options in this software, the coupling member surface with the line release option will be shown below. The structural system and the cross-section dimensions are shown in Figure 1.

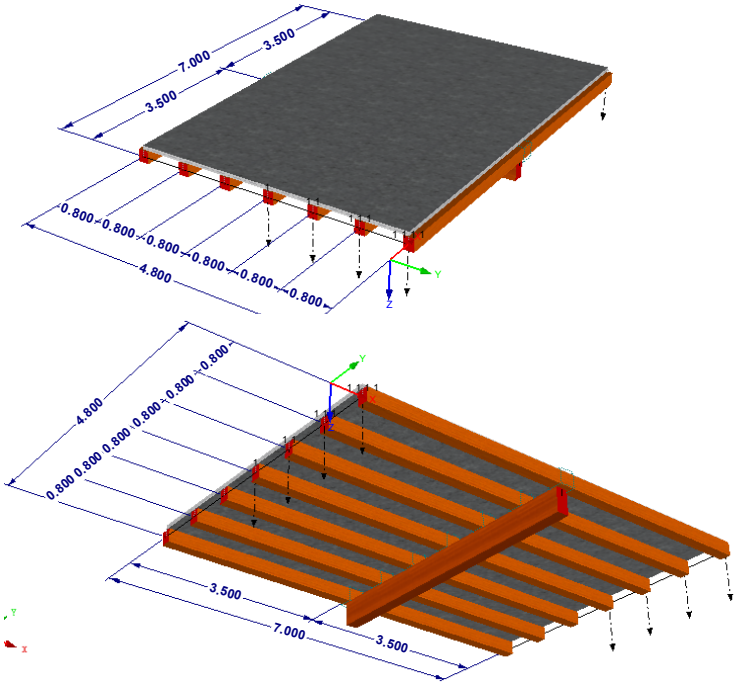


**Figure 1.** Structural system.

The model consists of timber elements that are defined as a member, with a given eccentricity. At the contact lines of wooden beams and concrete slabs, the line hinge is created. Thus, it is possible to release one of the components and to control the relation to each other by a line release type. The flexibility is considered by defining the spring constant. This method has proven to be very accurate in determining the internal forces and the effect of shrinkage, but the disadvantage is that the shear flow cannot be read directly, and the solution is shown below. This paper looks into the HBV-shear connector for a TCC system. Recently, the HBV-shear connector has gained popularity because it is the only connector to create a wide area connection that corresponds to slip modulus, which describes the efficiency of a connector, which is high compared to other connectors [65]. It is important to note that this only applies to serviceability classes 1 and 2, and concrete minimum class C20/25. It is recommended that the thickness of the concrete slab is 70 mm minimum. The effect of cracks on the bearing was taken into account, as well as the effect of creep and shrinkage. Finally, vibration analysis was performed.

### *3.1. Compliance of the Connection–$K_{ser}$*

An additional line is generated and it is associated with the concrete surface, while the lower line is associated with the timber member. The spring is defined accordingly to the degree of freedom (Figure 2).

According to abZ. Z-9.1-557, the calculated value of the initial displacement module (time t = 0) of an HBV shear connector (see Figure 3) per millimeter of expanded metal length may be assumed for the proof of usability with:

$K_{ser} = 825 - 250\ (d_{ZS})^{0.2}$ [N/mm] per mm of expanded metal length.

where $d_{ZS}$ is the thickness of the intermediate layer in mm. The calculated value of the initial displacement module of an HBV shear connector for the proof of the load-bearing capacity is 2/3 of the calculated value of the initial displacement module to accept the proof of usability. The displacement module of an HBV shear connector at the time $t = \infty$ may be assumed with 0.5 times the value at time t = 0.

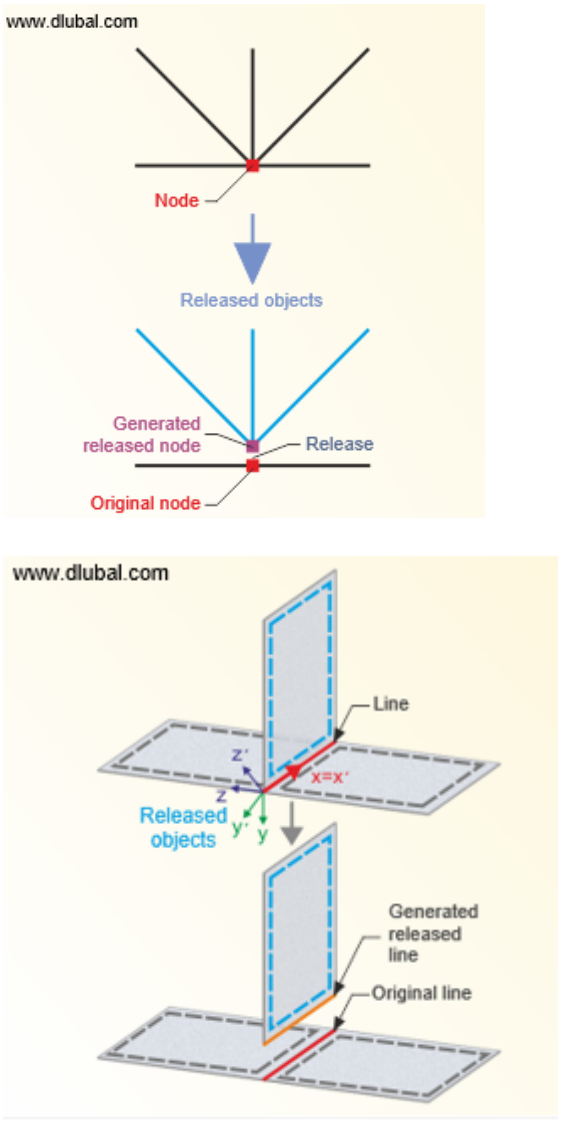


**Figure 2.** Nodal and line release.

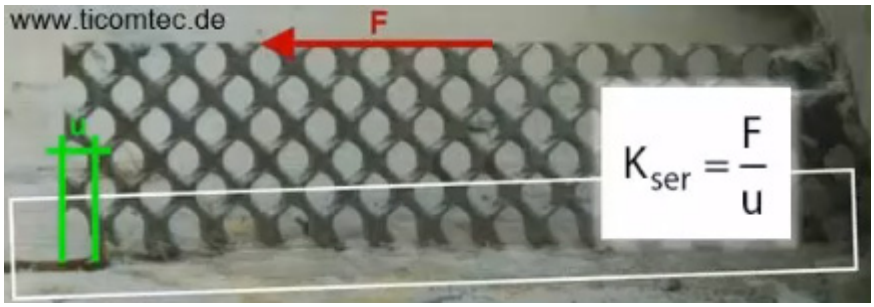


**Figure 3.** HBV connector–connection.

The characteristic load-bearing capacity $T_k$ of the HBV shear connectors with parallel loads to the expanded metal axis (longitudinal shearing) as follows:

$T_k = 160 - 8.0\ (d_{ZS})^{0.5}$ in N per mm of strip length.

The design value of the load-bearing capacity $T_d$ of the HBV shear connector may be taken as follows:

$$T_d = T_k/1.25 \quad (19)$$

In this case:

$$K_{ser} = 825 - 250 \cdot 20^{0.2} = 370{,}000 \text{ kN/m}^2 \quad (20)$$

$$T_d = (160 - 8 \cdot 20^{0.2})/1.25 = 100 \text{ kN/m} \quad (21)$$

The permanent and imposed load was determined following [66], while the shrinkage effect (Figure 4) was taken as follows [38]:

$$\Delta T = \varepsilon_{cs\,oo}/\alpha_T \quad (22)$$

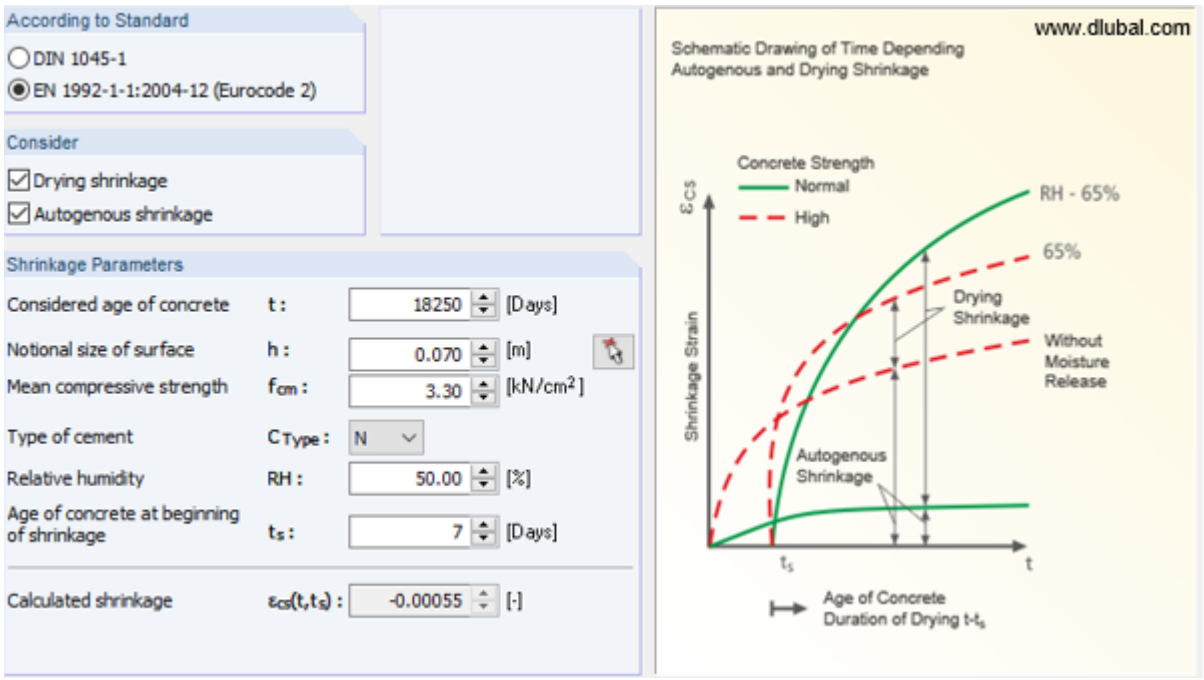


**Figure 4.** Shrinkage determination.

Finally, the load combinations [37] are made as follows:

$$w_{inst} = G + Q_1 + \sum[\![\psi_0 \cdot Q_{i,k}]\!] \quad (23)$$

$$w_{inst} = G + Q_1 \quad (24)$$

$$w_{net,fin} = G_{kdef} + \sum[\![\psi_2 \cdot Q_{i,k,def} - w_c]\!] \quad (25)$$

$$w_{net,fin} = G_{k,def} + \psi_2 \cdot Q_{1,kdef} \quad (26)$$

$$w_{fin} = Q_1 \cdot (1 - \psi_2) + \sum[\![Qi \cdot (\psi_0 - \psi_2) + G_{kdef} + \psi_2\, Q_{1,kdef}]\!] + \sum[\![\psi_2 \cdot Q_{i,kdef}]\!] \quad (27)$$

$$w_{fin} = Q_1 \cdot (1 - \psi_2) + G_{kdef} + \psi_2 \cdot Q_{1,kdef} \quad (28)$$

The difficulties occur when taking into account modified deformation, i.e., with reduced stiffness, and how to calculate it in a load combination. It means that the two separate combinations have to be taken into account and superimposed in a result combination (RC1). Given that it is a composite system and materials with different characteristics, in Tables 2 and 3 a stiffness reduction overview is given.

**Table 2.** Stiffness reduction.

| Limit State | Time | Timber | Concrete | Connector | LC |
|---|---|---|---|---|---|
| ULS | t = 0<br>t = ∞ | $E_{mean}$<br>$E_{mean}/(1 + k_{def})$ | $E_{cm}$<br>$E_{cm}/3.5$ | $2\ K_{ser}/3\ \gamma_M$<br>$0.5{\cdot}(2\ K_{ser})/(3\ \gamma_M)$ | LC1<br>LC2 |
| SLS | t = 0<br>t = ∞ | $E_{mean}$<br>$E_{mean}/(1 + k_{def})$ | $E_{cm}$<br>$E_{cm}/3{,}5$ | $K_{ser}$<br>$0.5{\cdot}K_{ser}$ | LC3<br>LC4, RC1 |

**Table 3.** Modification of stiffness by the multiplication factor.

| Material | The Factor for E, G | | |
|---|---|---|---|
| Poplar and Softwood Timber C24 | 0.625000 | | |
| Glulam Timber GL32h | 0.625000 | | |
| Concrete C25/30 | 0.285000 | | |
| **The Factor for Connector Stiffness** | | | |
| **Cux** | **Cuy** | **Cuz** | **Cφx** |
| 0.5 | 1.0 | 1.0 | 1.0 |

In this paper, the ability to implement reduced values in a relatively simple way was presented. Reduction of the stiffness is done as follows.

### *3.2. Results*

The process of designing and checking vibration and other construction requirements is shown in Figure 5.

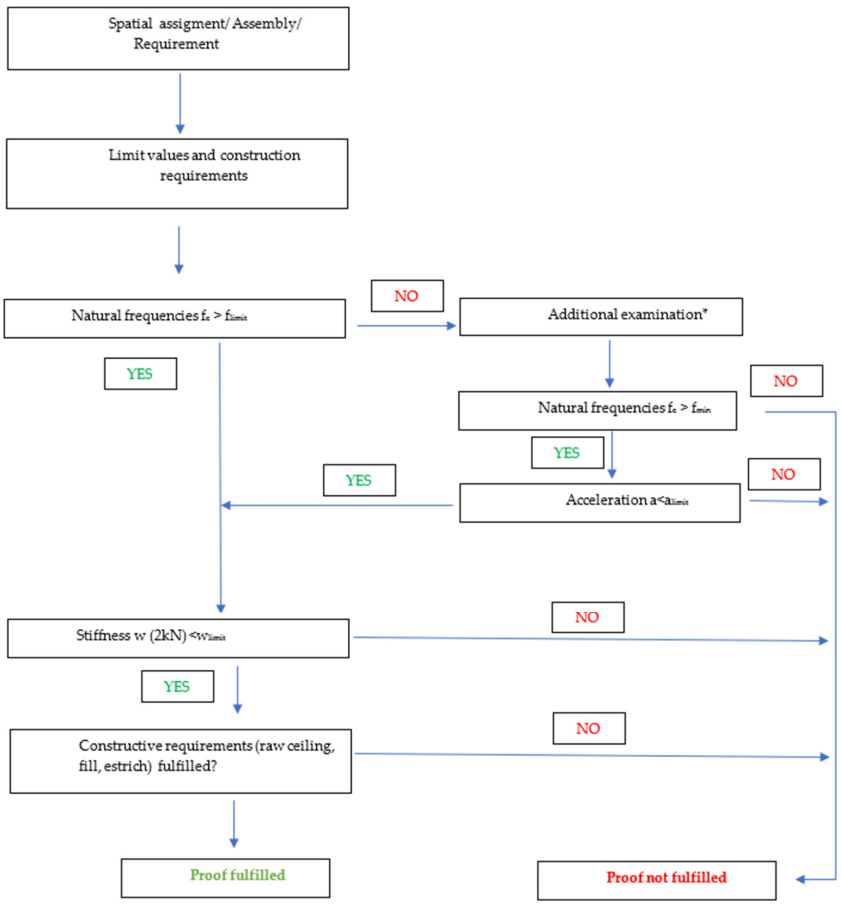


**Figure 5.** Decision tree. * The additional examination of acceleration is successful only in the case of timber–concrete composite systems, or other heavy systems with wide spans.

As it is a residential space, it is important to determine whether the condition of the allowed frequencies of the TCC floor slab are fulfilled. This part was done in a special module DYNAMPro (Figure 6), and the result is given in the tabular form (Table 4), where it is seen that the dominant first mode reaches 9.967 Hz, which is higher than the required 8 Hz so that the requirement is fulfilled.

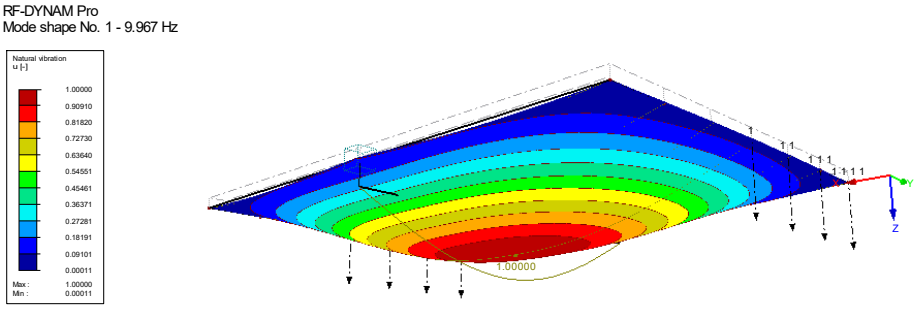


**Figure 6.** Natural frequencies of TCC floor.

**Table 4.** Natural frequencies.

| Mode | Eigenvalue | Angular Frequency | Natural Frequency | Natural Period |
|---|---|---|---|---|
| **No.** | **l [1/s$^2$]** | **v [rad/s]** | **f [Hz]** | **T [s]** |
| 1 | 3921.982 | 62.626 | 9.967 | 0.100 |
| 2 | 15,583.944 | 124.836 | 19.868 | 0.050 |
| 3 | 19,639.645 | 140.142 | 22.304 | 0.045 |
| 4 | 21,777.285 | 147.571 | 23.487 | 0.043 |

For practical use, the simplified natural frequency calculation rule is very useful. In this analysis, the deflection under permanent and quasi-permanent action at the ideal one-span beam may not exceed a limit value (6 mm according to DIN 1052). If the relationship shown in Figure 7 between natural frequency and deflection is considered for a hinged one-span beam that is subjected to a constant uniform load, then the 6 mm of deflection corresponds to a minimum natural frequency of about 7.2 Hz. Taking into account the fact that, in most National Annexes of EC 5, a minimum natural frequency of 8Hz is to be considered, a maximum deflection of about 5 mm is allowable. According to Figure 8 and the simplified method, frequency is higher than 8 Hz, so the postulate is fulfilled.

$$f_e \approx 5/\sqrt{(0.8 \cdot w(cm))} \approx 17.753/\sqrt{3} \quad (29)$$

$$w \approx 17.753/(f_e{}^2) \quad (30)$$

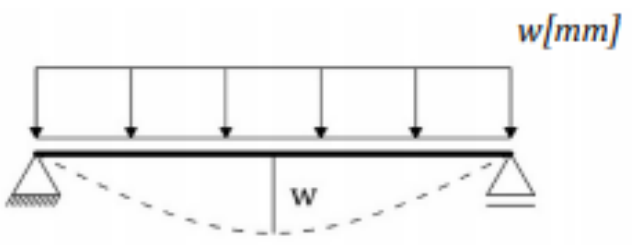


**Figure 7.** Simplified method.

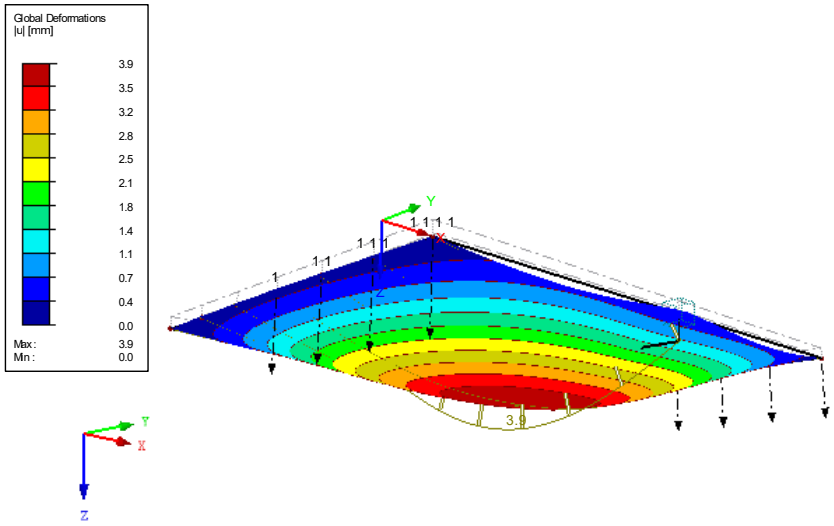


**Figure 8.** Global deformation of TCC floor.

### *3.3. Stiffness Design*

According to [19], the stiffness criterion is very important to check, because the frequency criterion alone is not sufficient. In this paper, the stiffness under a static load of 2 kN is checked. The deflection due to the load needs to be less than the deflection limit value. If the vibrations are noticeable only when you concentrate on them and are not annoying, then $w_{limit}$ = 0.5 mm. This is usually the case for floors in residential or office buildings. On the other hand, if the vibrations are quite noticeable, but not annoying, then $w_{limit}$ = 1.0 mm (e.g., family house). The analytical approach of this design is to create a replacement simple beam system, with an appropriate span corresponding to the largest range of the TCC floor. According to [19,67,68], the deflection may be calculated as follows:

$$w\ (2kN) = (2 \cdot l)/(48 \cdot EI_l \cdot b_{w(2kN)}) \leq w_{limit} \quad (31)$$

$$b_{w(2kN)} = \min\{(b_{ef}\ @\ b\ (\text{width of the floor})) \quad (32)$$

$$b_{ef} = l/1.1 \cdot \sqrt[4]{((EI_b/(EI_l) = b/(1.1 \cdot \alpha))} \quad (33)$$

Although in [34], for stiffness design, a static load of 1 kN was used and a substitutional static system, based on research and work [10]. In this paper, a load of 2 kN and the real TCC system were examined.

It is shown (Figure 9) that the deflection is obtained from 0.3 mm, which satisfies the requirements following [19].

$$0.03 < 0.5 \text{ mm} \quad (34)$$

### *3.4. Connector Design*

Lastly, special attention needs to be paid to the forces that occur in the connector, which are transferred from the member to the surface and conversely. To determine the shear flow, sections were made exactly at the intersection of the wooden elements and the concrete slab, ie., at the joint location.

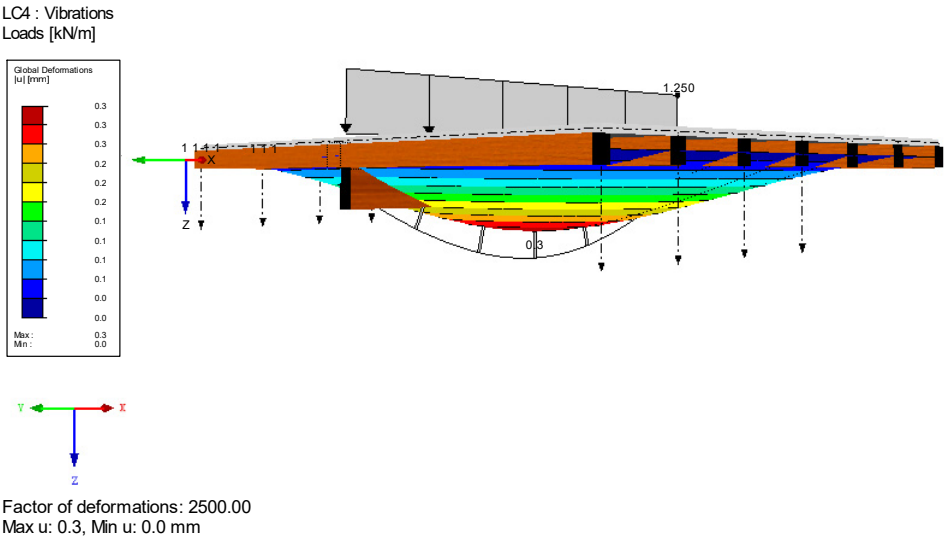


**Figure 9.** Deflection–stiffness design.

Observing the middle beam and superimposing the effect on both sides, in Figure 10, the total force is obtained. The average internal force amounts to 5.01 kN/m′, while the total force is 9.21 kN, which represents the average value multiplied by the length (Figure 11). The total force on the connector is 9.21 kN multiplied by 2 (both sides). After applying the same principle in the area of every connector, it can be concluded that the maximum force that occurs is less than the allowable previously calculated load capacity (21).

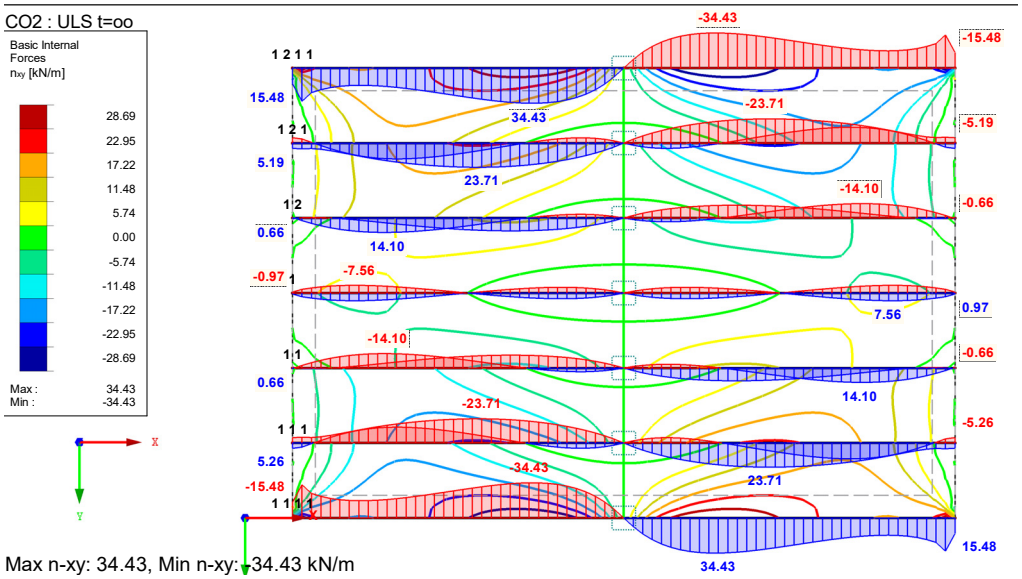


**Figure 10.** Shear flow.

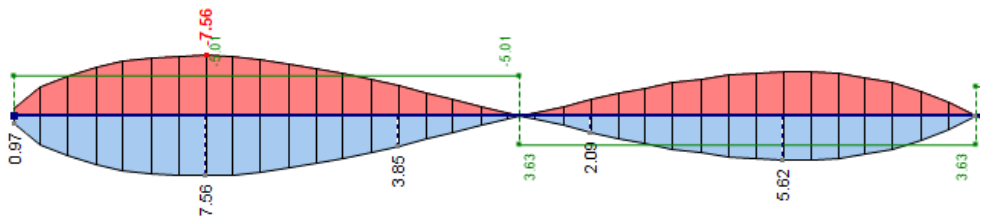

**Figure 11.** Sum and average internal force on the connector.

### *3.5. Concrete Check*

Stress analysis in concrete was performed. The tensile stress in the lower zone of the concrete slab was primarily checked according to EN 1992-1-1, NDP (7.2). The limitation of concrete compressive stress is $\sigma_{c,\,max}$ = 11.25 N/mm$^2$, and as Figure 12 shows, maximal stress in the TCC floor slab is 2.4 N/mm$^2$.

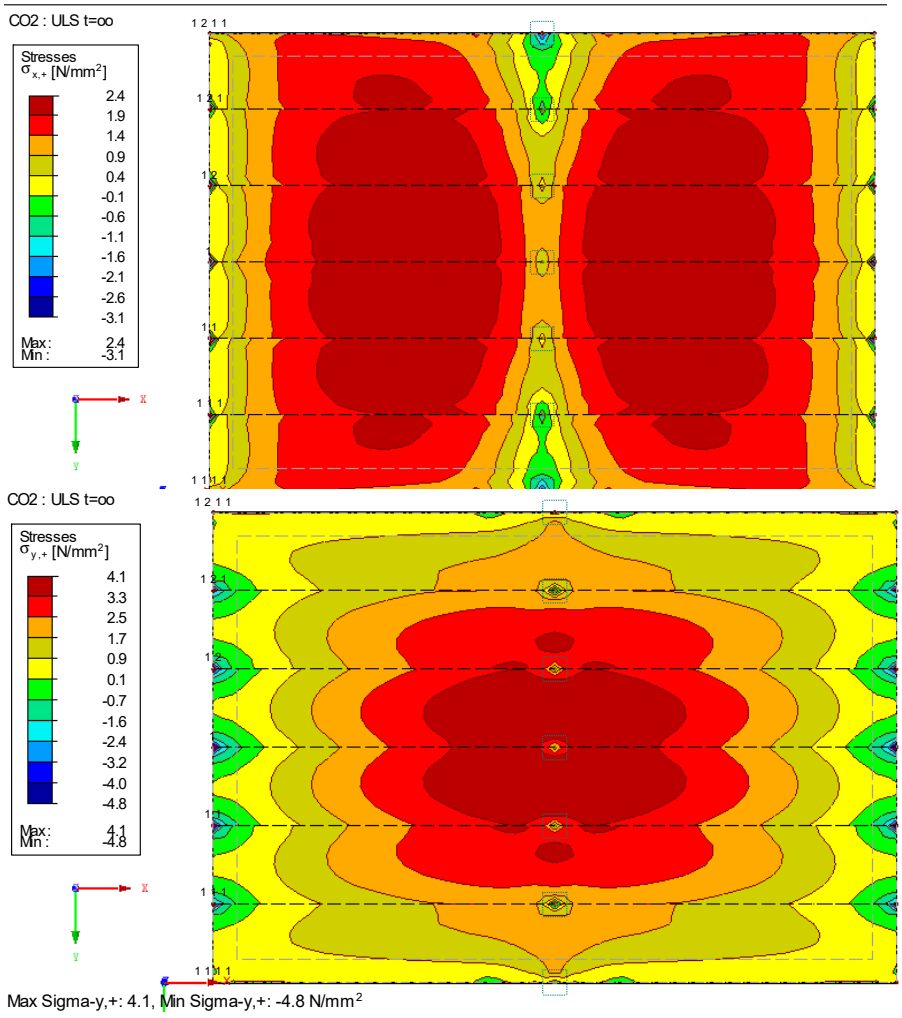


**Figure 12.** Concrete stresses.

### *3.6. Acceleration Design*

The additional examination of acceleration is successful only in the case of timber–concrete composite systems, or other heavy systems with wide spans. If the frequency is smaller than 8 Hz, an acceleration check is required. Empirical investigations in the 80 s offered the results that the vibration with a frequency lower than 8 Hz is dependent on the acceleration, and higher than 8 Hz is dependent on the velocity. The velocity check is not often considerable, because a typical timber floor is heavy enough (acoustic reasons), therefore, the velocity check is not relevant. The surface-to-surface model is shown in Figure 13.

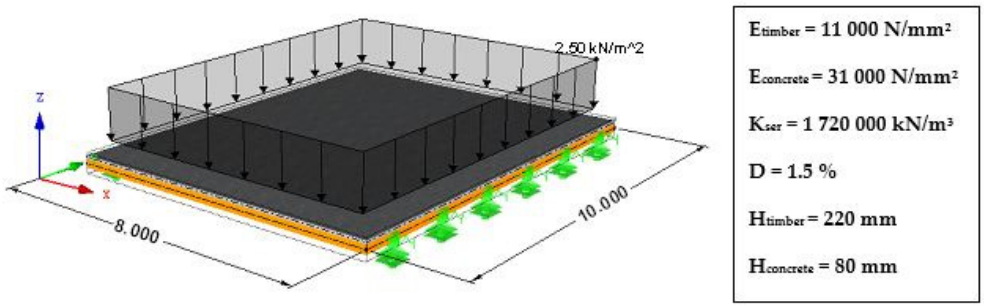


**Figure 13.** TCC Floor slab dimensions and characteristics.

After the dynamic calculation, the results show that the natural frequency, in this case, is 6.228 Hz, which is less than 8 Hz (see Table 5).

**Table 5.** Natural frequencies.

| Mode | Eigenvalue | Angular Frequency | Natural Frequency | Natural Period |
|---|---|---|---|---|
| **No.** | **l [1/s$^2$]** | **v [rad/s]** | **f [Hz]** | **T [s]** |
| 1 | 1561.041 | 39.510 | 6.288 | 0.159 |
| 2 | 1974.294 | 44.433 | 7.072 | 0.141 |
| 3 | 3402.945 | 58.335 | 9.284 | 0.108 |
| 4 | 6336.676 | 79.603 | 12.669 | 0.079 |

According to the analytical equation, acceleration is calculated as follows:

$$a = F_{dyn}/(M \cdot 2D) = (0.4 \cdot 1 \cdot 700\ N)/(m \cdot 0.5 \cdot l \cdot 0.5 \cdot b \cdot 2 \cdot D) = 56/(m \cdot l \cdot b \cdot D) \quad (35)$$

where:

- M—the modal mass of the TCC floor
- 700 N—harmonic part of the force (see [69])
- 0.1—Fourier coefficient
- 0.4—simplification factor (person moves around)
- m—mass (kg)
- l—TCC floor span (m)
- b—the width of the floor (<1.5 l)
- D—damping (following [70,71])

After the analysis, the results shown in Figure 14 indicates that the maximum acceleration at the relevant point occurs before the 10th second, and it is lower than the limit value of 0.05 m/s$^2$. Besides, the RMS value is displayed. For the floor to be deemed acceptable this value must be less than a limit based on the floor's fundamental natural frequency. However, RMS acceleration can only be used for more resonant excitation.

### *3.7. Constructive Design Requirements*

Since the vibration criterion is closely related to mass and stiffness, it is recommended to use heavy screeds and generally heavier layers, not less than 60 kg/m$^2$. In the illustrative example, Table 6 shows that the sum of the loads in the Z direction is equal to 119.27 kN. If this is divided by the total area of 7.0 × 4.8 m, it obtains a satisfactory weight of 354 kg/m$^2$, thus fulfilling this condition.

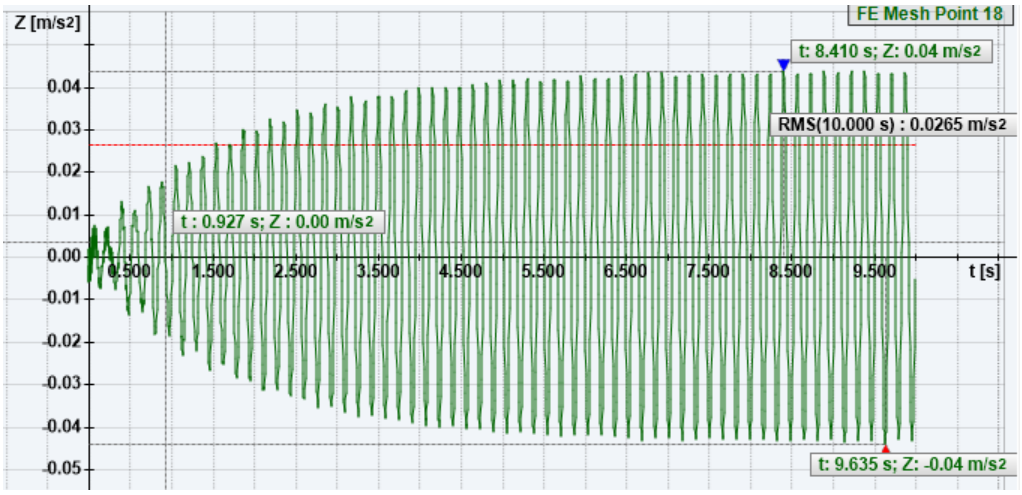


**Figure 14.** Acceleration in the relevant node.

**Table 6.** Sum of loads.

| Description | Value | Unit |
|---|---|---|
| **LC1—Permanent Load** | | |
| Sum of loads in X | 0.00 | kN |
| Sum of loads in Y | 0.00 | kN |
| Sum of loads in Z | 119.27 | kN |

### *3.8. Comparison Study*

When reviewing the existing literature, the difference in detailing steps for the calculation according to NDS 2018 and Eurocode 5 is noticeable. According to the results shown in [72], the main distinction between the two codes is where the deformation/creep factor is applied in the design process. Following the US calculation method, this factor is added at the end of the calculation and, consequently, affects only the deflections. On the other hand, EC5 applies the creep factor right at the beginning of the calculation to the modulus of elasticity. The long-term deflection shows the difference between the European and US method of calculations. The European method for long-term total load deflection is greater and more conservative than the US method [72]; therein lies the cause of the minor scattering of FEM results of this case study compared to certain results available in the literature.

Furthermore, the parametric analysis (software SAP 2000) shown in [73] was focused on the structural components of the TCC floor and the geometry of the floor. It can be concluded that timber joists were found to be the most influential on the natural frequency of the floor, and increasing the depth of the timber joists of TCC floors is the most effective means of increasing the floor's frequency.

Finally, the influence of the connector types on the behavior of the TCC system is highlighted. The reason for using the HBV connector for this case study is that HBV connectors have been shown to have about 10% better efficiency compared to mechanical fasteners (STS shear connectors) [74]. Finite element analysis and parametric study in [74] show that the thickness of the steel connector is closely related to the shear stiffness and strength of the TCC system. Another important conclusion useful in practice is that the gap between the concrete and timber, up to a certain width, does not affect the slip modulus of the connecting system, which leaves the space for the insulation material that can improve the vibration and sound performance of the TCC floor.

## 4. Discussion

Special attention should be paid to areas where there are larger slab spans or where there are higher loads. In this case, frequencies of less than 8 Hz occur, and then the acceleration requirement should be checked. However, EN 1995-1-1 does not prescribe special measures and conditions to be met. As a recommendation and plan for further research, it is proposed to see the influence of walls and boundary conditions of the TCC floor, and especially nonload-bearing walls influence of vibrations. Furthermore, the bending stiffness of a floating floor should be taken into account. There are a lot of technical topics and issues which need to be addressed and taken into account in the design process of TCC, which makes TCC a very exciting building component to design. Reviewing the differences between the Eurocode and North American codes, such as NDS 2018, the discrepancies are observed, and they need to be addressed and researched. Finally, there is a great variety of information and research on TCC connectors; therefore, a lot of further research can emerge from this paper, specifically with different connectors, finite element software analysis, and experimental testing.

## 5. Conclusions

This paper was intended to research TCC systems and their applications while focusing on FEM analysis and vibration performance of standard TCC systems in residential and office buildings, and potential problems that may occur related to vibration design. In addition to the proposed models for the calculation of vibration, velocity, and acceleration, analytical models for calculating different types of slip modulus are given. This is an important detail because the degree of coupling conditions the stiffness of the system and, thus, the vibration conditions themselves. The composite timber–concrete system is an efficient system that is applicable during new construction or restoration, and consists of a monolithic concrete slab connected to timber beams. Comparing the load-bearing capacity of this composite system with the load-bearing capacity of the constituent elements, it can be concluded that the system has up to four times higher stiffness and up to twice the load-bearing capacity. For wide-span ceilings, the vibration design is often governing. The advantage of the lighter material of timber over concrete becomes a disadvantage, because a high mass material is advantageous for a low natural frequency. Having long stiff support beams and shorter floor spans can ensure improved vibration performance when compared to systems with longer floor spans and shorter beam spans. An assessment and calculation of the TCC system was made, which was satisfactory for the frequency, additional acceleration, and stiffness limit criterion. Additionally, constructive design requirements are fulfilled. Finally, FE analysis showed that stresses occur locally within the connector area in the concrete slab on both sides of the joint. The advantages of TCC (vs. sole timber) that can be emphasized are increased stiffness through composite action, increased floor mass at decking level, improved sound insulation (airborne sound), and reduced sensitivity concerning vibrations. If, on the other hand, the TCC is compared with pure concrete, it can be concluded that the weight is reduced, the $CO_2$ emissions are reduced, the building process is faster, and reduced effort is needed for the props and formwork.

**Author Contributions:** Conceptualization, V.R., N.P. and J.B.; methodology, N.P. and J.B.; software, N.P.; validation, N.P.; formal analysis, V.R., N.P. and J.B.; investigation, J.B. and N.P.; resources, V.R., N.P. and J.B.; writing—original draft preparation, N.P. and J.B.; writing—review and editing, V.R., N.P. and J.B.; visualization, N.P.; conclusion, N.P.; supervision, V.R. All authors have read and agreed to the published version of the manuscript.

**Funding:** This research received no external funding.

**Institutional Review Board Statement:** Not applicable.

**Informed Consent Statement:** Not applicable.

**Data Availability Statement:** Data available on requzest due to restrictions eg privacy or ethical. The data presented in this stury are available on request from the corresponding author.

**Conflicts of Interest:** The authors declare no conflict of interest. The funders had no role in the design of the study; in the collection, analyses, or interpretation of data; in the writing of the manuscript, or in the decision to publish the results.

## References

1. Rajčić, V.; Žagar, Z. FEM models of composite timber-lightweight concrete floor systems. In Proceedings of the World Conference on Timber Engineering (WCTE 2000), Whistler, BC, Canada, 31 July–3 August 2000.
2. Yooh, D.; Fagiacomo, M.; De Franceschi, M.; Boon, K.H. State of the art on timber-concrete composite structures: Literature review. *J. Eng.* **2011**, *137*, 1085–1095. [CrossRef]
3. Klotz, S.; Holschemacher, K.; Köhler, S. Wirtschaftlichkeit von Holz-Beton-Verbunddecken. In *Holz-Beton-Verbund: Innovationen im Bauwesen, Beiträge aus Praxis und Wissenschaft*; König, G., Holschemacher, K., Dehn, F., Eds.; Bauwerk Verlag: Leipzig, Germany, 2004; pp. 269–279.
4. Newcombe, M.P.; Carradine, D.; Pampanin, S.; Buchanan, A.H.; Deam, B.L. In-plane experimental testing of timber-concrete composite floor diaphragms. In Proceedings of the NZSEE 2009 Conference, Christchurch, New Zealand, 3–5 April 2009.
5. Smith, I.; Frangi, A. *Use of Timber in Tall Multi-Storey Buildings*; IABSE: Zürich, Switzerland, 2014.
6. Movaffaghi, H.; Pyykkö, J.; Yitmen, I. Value-driven design approach for optimal long-span timber-concrete composite floor in multi-storey wooden residential buildings. *Civ. Eng. Environ. Syst.* **2020**, *37*, 100–116. [CrossRef]
7. Stepinac, M.; Šušteršič, I.; Gavrić, I.; Rajčić, V. Seismic design of timber buildings: Highlighted challenges and future trends. *Appl. Sci.* **2020**, *10*, 1380. [CrossRef]
8. Sebastian, W.; Webb, S.; Nagree, H.S. Orthogonal distribution and dynamic amplification characteristics of partially prefabricated timber-concrete composites. *Eng. Struct.* **2020**, *219*, 110693. [CrossRef]
9. Zhang, X.; Hu, X.; Gong, H.; Zhang, J.; Lv, Z.; Hong, W. Experimental study on the impact sound insulation of cross laminated timber and timber-concrete composite floors. *Appl. Acoust.* **2020**, *161*, 107173. [CrossRef]
10. Dias, A.M.P.G.; Skinner, J.; Crewa, K.; Tannert, T. Timber Concrete composites increasing the use of timber in construction. *Eur. J. Wood Wood Prod.* **2016**, *74*, 443–451. [CrossRef]
11. Dias, A.M.P.G.; Schänzlin, J.; Dietsch, P. *Hybrid Structures: State of Art Report*; Cost Action FP1402: Brussels, Belgium, 2017.
12. Knauf, M. Market potentials for timber-concrete composites in Germany's building construction sector. *Eur. J. Wood Wood Prod.* **2017**, *75*, 639–649. [CrossRef]
13. Andersson, J. *A Survey of Multi-Objective Optimization in Engineering Design*; LiTH-IKP-R-1097; Department of Mechanical Engineering Linköping University: Linköping, Sweden, 2000.
14. Weckendorf, J.; Toratti, T.; Smith, I.; Tannert, T. Vibration serviceability performance of timber floors. *Eur. J. Wood Wood Prod.* **2016**, *74*, 353–367. [CrossRef]
15. Dolan, J.D.; Murray, T.M.; Johnson, J.R.; Runte, D.; Shue, B.C. Preventing annoying wood floor vibrations. *J. Struct. Eng.* **1999**, *125*, 19–24. [CrossRef]
16. Talja, A.; Toratti, T. Effect on floating floors on the vibration performance of wood-concrete composite floors. In Proceedings of the World Conference on Timber Engineering (WCTE 2000), Whistler, BC, Canada, 31 July–3 August 2000.
17. Mertens, C.; Martin, Y.; Dobbels, F. Investigation of the vibration behaviour of timber-concrete composite floors as part of a performance evaluation for the belgian building industry. *Build. Acoust.* **2007**, *14*, 25–36. [CrossRef]
18. Abd Ghafar, N.H.; Deam, B.; Fragiacomo, M.; Buchanan, A. Vibration performance of LV-concrete composite floor systems. In Proceedings of the World Conference on Timber Engineering (WCTE 2008), Miyazaki, Japan, 2–5 June 2008.
19. Hamm, P.; Richter, A.; Winter, S. Floor vibrations: New results. In Proceedings of the World Conference on Timber Engineering (WCTE 2010), Trento, Italy, 20–24 June 2010.
20. Rijal, R.; Samali, B.; Crews, K.; Shrestha, R. Dynamic behaviour of timber-concrete composite flooring systems. In Proceedings of the World Conference on Timber Engineering (WCTE 2010), Trento, Italy, 20–24 June 2010.
21. Skinner, J.; Harris, R.; Paine, K.; Walker, P.; Bregulla, J. The characterisation of connectors for the upgrade of timber floors with thin structural toppings. In Proceedings of the World Conference on Timber Engineering (WCTE 2012), Auckland, New Zealand, 15–19 July 2012.
22. Omenzetter, P.; Kohli, V.; Desgeorges, Y. Evaluation of timber-concrete floor performance under occupant-induced vibrations using continuous monitoring. *Key Eng. Mater.* **2013**, *569–570*, 230–237. [CrossRef]
23. Fong, L.Y.; Abd Ghafar, N.H.; Abd Rahman, N.; Fragiacomo, M.; Ibrahim, Z.; Buchanan, A. Comparison between the vibration performance of LVL-concrete composite (LCC) flooring system made of Malaysian and New Zealand LVL. *Malays. J. Civil Eng.* **2015**, *27*, 68–80.
24. Dos Santos, P.G.G.; Martins, C.E.J.; Skinner, J.; Harris, R.; Dias, A.M.P.G.; Godinho, L.M.C. Modal frequencies of a reinforced timber-concrete composite floor: Testing and modeling. *J. Struct. Eng.* **2015**, *141*, 04015029. [CrossRef]
25. Kozarić, L. Vibrations of repaired wooden floors caused by human action. *Wood Res.* **2015**, *60*, 663–670.
26. Marshall, E.J.N.; Granello, G.; Palermo, A. Vibration performance of timber-concrete composite floors: A case study. *J. Struct. Eng. Soc. N. Z. Inc.* **2020**, *33*, 33–46.

27. Mushina, J.; Abd Ghafar, N.H.; Yeoh, D.; Mushina, W.; Boon, K.H. Vibration behaviour of natural timber and timber concrete composite deck ystem. *Mater. Sci. Eng.* **2020**, *713*, 012023.
28. Jarnerö, K. Vibrations in Timber Floors: Dynamic Properties and Human Perception. Ph.D. Thesis, Linnaeus University, Växjö, Sweden, 2014.
29. CEN/TC 250. *Technical Specification—Background Document—Eurocode 5: Design of Timber Structures—Vibrations*; CEN: Brussels, Belgium, 2020.
30. ISO. *Bases for Design of Structures: Serviceability of Buildings and Walkways against Vibrations*; ISO 10137:2007; ISO: Geneva, Switzerland, 2007.
31. CEN. *Eurocode 0: Basis of Structural Design*; EN 1990:2002+A1:2005+A1:2005/AC:2010; CEN: Brussels, Belgium, 2010.
32. Ohlsson, S.V. *Svikt, svängningar och styvhet hos bjälklag: Dimensioneringsregler*; Rapport T20; BFR: Stockholm, Sweden, 1984.
33. CEN/TC 250. *Technical Specification—Background Document—Eurocode 5: Design of Timber Structures—Structural Design of Timber-Concrete Composite Structures—Common Rules and Rules for Buildings*; CEN: Brussels, Belgium, 2020.
34. CEN. *Eurocode 5: Design of Timber Structures—Part 1-1: General-Common Rules and Rules for Buildings*; EN 1995-1-1:2004+AC:2006+A1:2008; CEN: Brussels, Belgium, 2008.
35. Pavic, A.; Reynolds, P. Vibration serviceability of long-span concrete building floors—Part 1: Review of background information. *Shock Vib. Dig.* **2002**, *34*, 191–211.
36. Pavic, A.; Reynolds, P. Vibration serviceability of long-span concrete building floors—Part 1: Review of mathematical modelling approaches. *Shock Vib. Dig.* **2002**, *34*, 279–297.
37. CEN. *Eurocode 4: Design of Composite Steel and Concrete Structures—Part 1-1: General Rules and Rules for Buildings*; EN 1994-1-1:2004+AC:2009; CEN: Brussels, Belgium, 2009.
38. CEN. *Eurocode 2: Design of Concrete Structures—Part 1-1: General Rules and Rules for Buildings*; EN 1992-1-1:2004+AC:2010; CEN: Brussels, Belgium, 2010.
39. Rieg, A. Verformungsbezogene mittragende Breite niedriger Verbundträger. Ph.D. Thesis, University of Stuttgart, Institute for Structural Design, Stuttgart, Germany, 2006.
40. Kuhlmann, U.; Merkle, J.; Schänzlin, J.; Bux, H. *Brettstapel-Beton-Verbunddecken mit integrierten Slim-Floor-Profilen*; Deutsche Bundesstiftung Umwelt AZ 211682006; Institute for Structural Design, University of Stuttgart: Stuttgart, Germany, 2006.
41. Xie, Z.; Hu, X.; Du, H.; Zhang, X. Vibration behavior of timber-concrete composite floor under human-induced excitation. *J. Build. Eng.* **2020**, *32*, 101744. [CrossRef]
42. Abd Ghafar, N.H.; Deam, B.; Fragiacomo, M. Vibration susceptibility of multi-span lvl-concrete composite floors. In Proceedings of the World Conference on Timber Engineering (WCTE 2010), Trentino, Italy, 20–24 June 2010.
43. Skinner, G.J. *Short Term Scientific Mission: The Vibration Performance of Round Wood Timber-Concrete Composite floors*; Cost Action FP1004: Brussels, Belgium, 2012.
44. Rijal, R. Dynamic Performance of Timber and Timber-Concrete Composite Flooring Systems. Ph.D. Thesis, Sydney University of Technology, Faculty of Engineering and Information Technology, Sydney, Australia, 2013.
45. Skaare, M.K. Vibrations in Composite Timber-Concrete Floor Systems. Master's Thesis, Norwegian University of Science and Technology, Trondheim, Norway, 2013.
46. Franklin, K.; Hough, R. Modelling and measurement of the dynamic performance of a timber concrete composite floor. In Proceedings of the World Conference on Timber Engineering (WCTE 2014), Quebec City, QC, Canada, 10–14 August 2014.
47. Rijal, R.; Samali, B.; Shrestha, R.; Crews, K. Experimental and analytical dtudy on dynamic performance of timber-concrete composite beams. *Constr. Build. Mater.* **2015**, *75*, 46–53. [CrossRef]
48. Abd Ghafar, N.H. Dynamic Behaviour of LVL-Concrete Composite Flooring Systems. Ph.D. Thesis, University of Canterbury, Christchurch, New Zealand, 2015.
49. Hu, L.; Auclair, S.C.; Chui, Y.; Ramzi, R.; Gagnon, S.; Mohammad, M.; Ni, C.; Popovski, M. Design method for controlling vibrations of wood-concrete composite floors systems. In Proceedings of the World Conference on Timber Engineering (WCTE 2016), Vienna, Austria, 22–25 August 2016.
50. Murray, T.M.; Allen, D.E.; Ungar, E.E. *Design Guide 11: Vibrations of Steel-Framed Structural Systems Due to Human Activity Second Edition 11 Steel Design Guide*, 2nd ed.; American Institute of Steel Construction: Chicago, IL, USA, 2016.
51. CEN. *Test Methods—Timber Flooring Systems: Determination of Vibration Properties*; EN 16929:2018; CEN: Brussels, Belgium, 2018.
52. Wyatt, T.A. *Design Guide on the Vibration of Floors*; Steel Construction Institute: Ascot, UK, 1989.
53. Murray, T.M.; Allen, D.E.; Ungar, E.E. *Steel Design Guide Series 11: Floor Vibrations Due to Human Activity*; American Institute of Steel Construction: Chicago, IL, USA, 1997.
54. Girhammar, U.A. A simplified analysis method for composite beams with interlayer slip. *Int. J. Mech. Sci.* **2009**, *51*, 515–530. [CrossRef]
55. Niederer, A. Grenzen der Anwendung des $\gamma$-Verfahrens. Bachelor's Thesis, HTWG Konstanz, Konstanz, Germany, 2008.
56. Grosse, M.; Hartnack, R.; Lehmann, S.; Rautenstrauch, K. Modellierung von diskontinuierlich verbundenen Holz-Beton-Verbundkonstruktionen. *Bautechnik* **2003**, *80*, 534–541, 693–701. [CrossRef]
57. Michelfelder, B.C. Trag- und Verformungsverhalten von Kerven bei Brettstapel-Beton-Verbunddecken. Ph.D. Thesis, University of Stuttgart, Institute for Structural Design, Stuttgart, Germany, 2006.

58. Ceccotti, A.; Fragiacomo, M.; Giordano, S. Long-term and collapse tests on a timber-concrete composite beam with glued-in connection. *Mater. Struct.* **2007**, *40*, 15–25. [CrossRef]
59. Lukaszewska, E.; Fragiacomo, M.; Frangi, A. Evaluation of the slip modulus for ultimate limit state verifications of timber-concrete composite structures. In Proceedings of the CIB-W18 no. 40, Bled, Slovenia, 28–31 August 2007.
60. Dias, A.M.P.G.; Cruz, H.M.P.; Lopes, S.M.R.; van de Kuilen, J.-W. Stiffness of dowel-type fasteners in timber-concrete joints. *Struct. Build.* **2010**, *163*, 257–266. [CrossRef]
61. Dias, A.M.P.G. Performance of dowel-type fasteners for hybrid timber structures. In Proceedings of the International Conference on Connections in Timber Engineering: From Research to the Standards, Graz, Austria, 13 September 2017.
62. Turrini, G.; Piazza, M. Una tecnica di recupero statico dei solai in legno. *Recuperare* **1983**, *2*, 5–7.
63. DIBT. *HBV-Schubverbinder aus Streckmetall und vorgefertigte Bauteile mit eingeklebten HBV-Schubverbindern für ein Holz-Beton-Verbundsystem*; DIBT: Berlin, Germany, 2020.
64. Kudla, K. *Short Term Scientific Mission: Notched Connections for TCC Structures*; Cost Action FP1402: Brussels, Belgium, 2017.
65. Deutsches Institut fur Bauctechnik. *Allgemeine Bauaufsichtliche Zulassung*; Zulassungsnummer Z-9.1-557; DIBT: Berlin, Germany, 2020.
66. CEN. *Eurocode 1: Actions on Structures—Part 1-1: General Actions—Densities, Self-Weight and Imposed Loads for Buildings*; EN 1991-1-1:2002+AC:2009; CEN: Brussels, Belgium, 2009.
67. Hamm, P. Schwingungsverhalten von decken bei auflagerung auf unterzügen. *Holzbau Die Neue Quadriga* **2008**, *526*, 41–46.
68. Maier, C.; Heger, C.; Neujahr, M.; Stöffler, J. *Großversuch zum Einfluss nichttragender Ausbauelemente auf das Schwingungsverhalten weitgespannter Verbundträger: Forschungsbericht*; Technical University of Darmstadt: Darmstadt, Germany, 2005.
69. Bachmann, H.; Ammann, W.J.; Deischl, F.; Eisenmann, J.; Floegl, I.; Hirsch, G.H.; Klein, G.K.; Lande, G.J.; Mahrenholtz, O.; Natke, H.G.; et al. *Vibration Problems in Structures: Practical Guidelines*, 2nd ed.; Birkhäuser Verlag: Basel, Switzerland, 1997.
70. SIA. *Holzbau—Ergänzende Festlegungen*; 265/1; SIA: Zürich, Switzerland, 2018.
71. Blaß, H.J.; Ehlbeck, J.; Kreuzinger, H.; Steck, G. *Erläuterungen zu DIN 1052: 2004-08: Entwurf, Berechnung und Bemessung von Holzbauwerken*; DGfH Innovations und Service GmbH: Munich, Germany, 2004.
72. Collins, L. Timber-Concrete Composite: An Alternative Composite Floor System. Master's Thesis, Kansas State University, Manhattan, KS, USA, 2020.
73. Marshall, J. Footfall Vibration Modelling and In-Situ Testing of Timber Concrete Composite Floors. Master's Thesis, University of Canterbury, Christchurch, New Zealand, 2020.
74. Al-Sammari, A.T.; Clouston, P.L.; Brena, S.F. Finite-element analysis and parametric study of perforated steel plate shear connectors for wood-concrete composites. *J. Struct. Eng.* **2018**, *144*, 04018191. [CrossRef]